

Isotropic – Liquid Crystalline Phase Diagram of A CdSe Nanorod

Solution

Liang-shi Li¹, Malgorzata Marjanska², Gregory H. J. Park, Alexander Pines, and A. Paul Alivisatos*

Department of Chemistry, University of California, Berkeley

Materials Sciences Division, Lawrence Berkeley National Laboratory

Berkeley, CA 94720

Abstract

We report the isotropic-liquid crystalline phase diagram of 3.0 nm × 60 nm CdSe nanorods dispersed in anhydrous cyclohexane. The coexistence concentrations of both phases are found to be lower and the biphasic region wider than the results predicted by the hard rod model, indicating that the attractive interaction between the nanorods may be important in the formation of the liquid crystalline phase in this system.

*To whom correspondence should be addressed. Email: alivis@uclink4.berkeley.edu

¹Present address: Chemistry Department, Northwestern University, 2145 Sheridan Road, Evanston, IL 60208-3113. ²Present address: Center for Magnetic Resonance Research, University of Minnesota, 2021 6th Street SE, Minneapolis, MN 55455.

I. Introduction

In concentrated solutions of rodlike particles dispersed in non-mesogenic solvents, it has been well accepted that the hard rod repulsion plays a predominant role^{1,2,3} in the formation of the liquid crystalline phases. Theoretical analyses incorporating the anisotropic attractive interaction between the rigid rods predict much more complex phase diagrams^{4,5}, such as the coexistence of two nematic phases, and even two isotropic phases, as well as the appearance of temperature dependent transition densities.

Lyotropic liquid crystalline solutions of rodlike viruses such as tobacco mosaic virus⁶ and fd-virus⁷ in water have been widely studied as model systems for hard rods. The electrostatic repulsion between the rods makes the effect of van der Waals interaction insignificant. On the other hand, it can be expected that van der Waals interaction may be important in inorganic colloidal systems with anisotropic shapes⁸ because of their high electron density and therefore high polarizability, especially in non-aqueous solutions where electric repulsion is not present. Boehmite rods (AlOOH) have been the only uncharged rigid rodlike colloidal system for which a liquid crystalline phase diagram has been reported⁹. Because the available AlOOH samples are highly polydisperse, however, and the phase diagram depends on the rod lengths, the experimental studies of that system cannot determine the boundaries of the isotropic-nematic coexistence region as a function of size. Indeed, the coexistence concentrations of the isotropic and nematic phases were found to be dependent on the total concentration, and therefore it is not a simple matter to compare to the hard rod model with attractions built in.

We have recently observed the formation of liquid crystalline phases of highly monodisperse semiconductor nanorods at high density in non-polar solvent¹⁰. The CdSe nanorods can be made with variable aspect ratio and tightly controlled widths and lengths, and the rods are not highly charged, so they are an interesting system to study the formation of lyotropic liquid crystals with attractive interaction included. Here we report a preliminary experimental study of the phase diagram of the nanorod solution.

II. Experiment

CdSe nanorods studied in this work are synthesized using previously published methods^{11,12}. The nanorods are characterized as 3.0 nm wide and 60 nm long with transmission electron microscopy (TEM), with $\sim 5\%$ width distribution and $\sim 15\%$ length distribution. The nanorods are coated with organic molecules, which not only make the nanorods very dispersible in organic solvent, but also change the effective dimensions of the nanorods in solution.

To make liquid crystalline solutions of nanorods, the nanorods are dissolved in anhydrous cyclohexane. The solution is then concentrated by blowing dry N_2 to evaporate the solvent. When it is concentrated enough to have birefringent droplets, the solution is transferred to 300 μm glass capillaries or 4 mm NMR tubes, which are then flame sealed for phase separation. The manipulation has to be done in a water free environment, because it was found that even the water vapor in air could cause gelation in the concentrated solution, which is presumably due to the reduction of the solvating power of the solvent.

The coexistence concentrations of the isotropic and the liquid crystalline phases at room temperature (25 °C) are determined with elemental analysis. Nanorod (3.0×60 nm) solutions with different compositions sealed in 300 μm diameter cylindrical glass tubes (10 μm wall thickness) are set aside for ~ 2 months until the completion of the phase separation, as shown in figure 1. Then the glass tubes were immersed in mineral oil (for refractive index matching), and digital images were taken under an optical polarizing microscope, so that the volume of each phase can be measured. The glass tubes are then cut at the phase boundaries, and the two phases separately collected. The cadmium content is determined with the standard inductively coupled plasma (ICP) technique after the nanocrystals are digested in acid, and therefore the concentration of CdSe can be calculated.

The isotropic–biphasic boundary is determined by varying the temperature of the solutions with different compositions under an optical polarizing microscope until the disappearance or appearance of the liquid crystalline phase. Once the isotropic-biphasic boundary is established, the biphasic-nematic boundary can be determined by measuring the isotropic-nematic volume ratio at different temperatures, using the characteristic difference in nuclear magnetic resonance (NMR) spectra of deuterium (^2H) nuclei in a probe molecule present in the isotropic or the liquid crystalline phases¹³. Anhydrous deuterated chloroform (C^2HCl_3) is added to the biphasic solution of the nanorods in anhydrous cyclohexane ($\sim 5\%$ by volume) in a 4 mm diameter glass NMR tube, and the NMR spectra were taken with a Chemagnetics Infinity 500 MHz spectrometer equipped with a 4 mm MAS solid state probe at temperatures ranging from room temperature to 75 °C. The temperature is varied by blowing compressed air of different temperatures over

the sample. Temperature calibration was performed with ethylene glycol ((CH₂OH)₂)^{14,15}, where the chemical shift difference between the protons in CH₂ and OH groups was measured at different temperature and compared with references. For each temperature, the sample was allowed to stabilize for 6 to 8 hours so that the spectra do not change with time. Because the C²HCl₃ probes the local order of the environment, there is no need to wait for the complete phase separation at different temperatures. The ²H-NMR spectra are shown in figure 2(A), where the central peak is identified to be due to the isotropic phase and the two side peaks to the liquid crystalline phase. The volume ratio of the two phases is calculated by the ratio of the areas under the corresponding peaks, by assuming the partition of chloroform in two phases is solely determined by the volumes of cyclohexane, and thus we can calculate the biphasic-nematic phase boundary with the lever rule.

III. Results and Discussions

The volume percentage of CdSe in the isotropic and the liquid crystalline phases at room temperature (25 °C) is determined to be 6.1% and 9.9%, respectively with the ICP technique. These values do not vary significantly ($\pm 0.4\%$) for solutions with different compositions, indicating the nanorods are monodisperse enough that the solution can be considered to be a two-component system, in contrast to the experiments reported for boehmite rods earlier⁹. This also allows the determination of the composition of any biphasic solution non-destructively from the volume ratio of the two phases.

For a solution with a composition of 6.5 % (volume percentage) of CdSe in cyclohexane, heating from 25 °C to 75 °C does not cause the disappearance of the


nematic phase, and therefore we conclude that the isotropic-biphasic boundary is independent of temperature within 0.4%. When considering the thermal expansion of the solvent that slightly decreases the concentration, the uncertainty in this boundary should be smaller for higher temperatures.

The volume ratio of the isotropic and liquid crystalline phases for a biphasic solution is calculated from ^2H -NMR spectra and shown in figure 2 (B), from which together with the isotropic-biphasic boundary the biphasic-nematic phase is calculated with the lever rule.

In order to compare with the theoretical results reported, however, the thickness of organic molecules (1.1 nm for two layers)¹⁶ on the nanorod surface is added to get the effective dimensions of the nanorods, which gives 4.1 nm in width, and 60 nm in length. The temperature vs. composition phase diagram, which is only weakly dependent on temperature in the temperature range studied, is thus drawn with the effective volume ratio, as shown in figure 3. The theoretical results for hard spherocylinders of aspect ratio of 15 calculated with the hard rod model^{17, 18} are also shown for comparison.

Within the temperature range studied (limited by the freezing and boiling points of cyclohexane), the discrepancies between our experimental and the theoretically calculated hard rod results are evident. Our experimental values for the coexistence concentrations are significantly lower than 19.2% and 21.5%, the coexistence concentrations calculated for hard spherocylinders of aspect ratio of 15 by assuming the hard rod repulsion alone between the nanorods^{17, 18}. As the aspect ratio becomes larger, the hard rod model does predict that the coexistence region shifts to lower concentrations

and broadens (see for instance reference 18, Figure 12). This means that by treating the aspect ratio as a completely adjustable parameter, it is possible to bring the calculated hard rod phase diagram into somewhat better agreement with the experiment. However, this occurs for an aspect ratio that is outside the range of what is measured by TEM, and even under these circumstances, the biphasic region measured experimentally remains wider than the calculated one. The ratio between the measured concentrations between the ordered and disordered phases is 1.62 at room temperature, which is significantly larger than the theoretically predicted value (~ 1.24) even for infinitely long, thin rods^{17, 18}.

A likely source of these discrepancies is the anisotropic attractive interactions between the nanorods. Theoretical studies on the rodlike colloids with attractive interactions^{4,5,19} have shown that introducing an orientation-dependent attractive potential results in the widening of the isotropic-nematic coexistence region, which is qualitatively  consistent with our experimental results. The presence of the inter-particle attraction makes the solute-solvent interaction parameter² more positive, so that the mixing becomes less enthalpically favorable, and consequently the concentration difference between the solute-rich and the solvent-rich phases increases². Furthermore, because the anisotropic part of the attractive interaction favors the parallel orientation between the rods, the anisotropic phase starts to appear at concentrations lower than those required by the hard rod repulsion. However, whether the coexistence concentration of the ordered phase is larger or smaller compared with the hard rod systems depends on the nature and the range of the attractive interaction, as shown by numerical calculations¹⁹.

Future studies will require a much more comprehensive study of the phase diagrams for rods of varying length and diameter, and in a solvent that permits a wider range of temperature to be investigated, as well as comparisons to models including different types of attractive interactions. The effect of van der Waals interaction in liquid crystals has been theoretically studied in the mean field approximation^{4,5,20,21,22}. However, considering the highly anisotropic polarizability of the nanorods as well as their permanent electric dipole moment along their long axes^{23,24,25}, both of which contribute to the attractive interaction, we may suspect whether the mean field treatment is still valid. Theoretically it was shown²⁶ that as soon as the attractive interaction mildly alters the second virial coefficient, the effect on the third virial coefficient is considerable. By assuming the attractive potential has the form of the van der Waals interaction at intermediate distances, the authors estimated that the contributions to the second virial coefficient from the attractive interaction and the hard rod repulsion respectively have a ratio $\sim \frac{4}{5} H^{-2} P^{-5} e^{HP}$, where P is the aspect ratio of rods, $H = \frac{3\pi A}{128k_B T}$, with A the Hamaker constant, k_B the Boltzmann constant and T the temperature. With the Hamaker constant for CdSe in cyclohexane of $0.5 \times 10^{-19} \text{ J}$ ²⁷, we estimate that for CdSe nanorods with aspect ratio of 15, the contribution to the second virial coefficient from the van der Waals interaction is ~ 0.7 of that from the hard rod repulsion and therefore not negligible. This indicates that in our system van der Waals interaction may be so important that the mean field treatment is no longer satisfactory. The large van der Waals attraction may also be the reason behind the gelation in the solution of nanorods in poor solvent, which has been suggested²⁸ for the gelation in aqueous suspension of V_2O_5 nanoribbons with

high salt concentration where the electrostatic repulsion cannot compensate van der Waals attraction effectively.

IV. Summary

We have measured the phase diagram of $3.0 \text{ nm} \times 60 \text{ nm}$ CdSe nanorods dispersed in cyclohexane. Only weak temperature dependence has been observed in the temperature range studied. In addition, the coexistence concentrations of the order and disordered phases are much lower than those predicted with the hard rod model, and the biphasic region is wider. We believe these discrepancies may result from the attractive interaction between the nanorods.

So far we have only measured the phase diagram of one CdSe nanorod sample in a very narrow temperature range. Expanding the experimental temperature range is currently in progress, as well as the determination of the phase diagram for nanorods with different widths and lengths. Because van der Waals interaction largely depends on the distance between the nanorods, by varying the sizes and aspect ratios of the nanorods, we can better understand the contribution of the attractive interactions, as well as the applicability of the van der Waals mean field theory in these systems. In addition, systematic study of the phase diagram of CdSe nanorods and comparison with results from numerical simulations can yield the information about the nature of the interaction of the nanorods with each other and with solvents, which is also instructive for selecting the most suitable experimental conditions for spatially manipulating these functional nanorods in fabricating electro-optical devices.



Acknowledgement

We thank the analytical facility of the College of Natural Resources at UC Berkeley for the use of the ICP spectrometer and Paul Brooks for the assistance. This work was supported by the Director, Office of Science, Office of Basic Energy Sciences, Division of Materials Sciences and Engineering of the U.S. Department of Energy under Contract No. DE-AC03-76SF00098 and by the Air Force Office of Scientific Research under Grant No. F49620-01-1-0033.

Figure captions

Figure 1. Completion of isotropic–liquid crystalline phase separation in the solution of 3.0 nm wide and 60 nm long CdSe nanorods in anhydrous cyclohexane observed between two parallel (A) and crossed (B) polarizers. The top layer is clear and isotropic, while the bottom phase is translucent and anisotropic. The color is due to the band edge absorption of the nanorods.

Figure 2. (A) Deuterium NMR spectra of C^2HCl_3 in doped biphasic CdSe nanorod solution at different temperatures. The central peak is due to the isotropic phase, and the two side peaks are due to the liquid crystalline phase. (B) The volume ratio of the two phases calculated from the areas under the corresponding peaks. The room temperature value is also shown (the spectrum not shown in A). The solid line is the polynomial fit of the data points.

Figure 3. The temperature vs. composition phase diagram in the temperature range studied (solid lines) after the organic surfactant molecules are considered. The dashed lines are the calculated values for hard spherocylinders of aspect ratio of 15 in *ref.* 17.

Figure 1

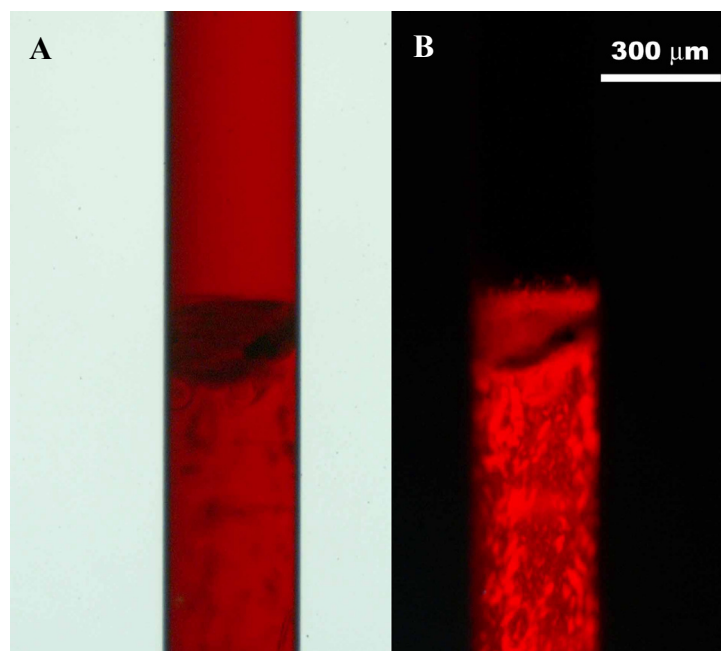


Figure 2

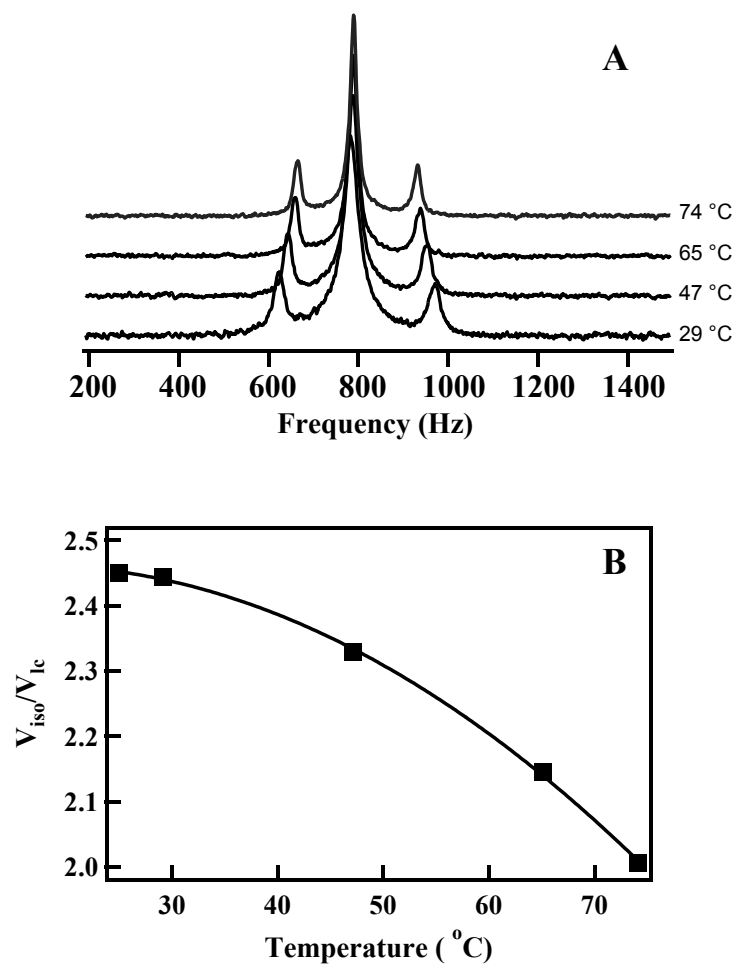
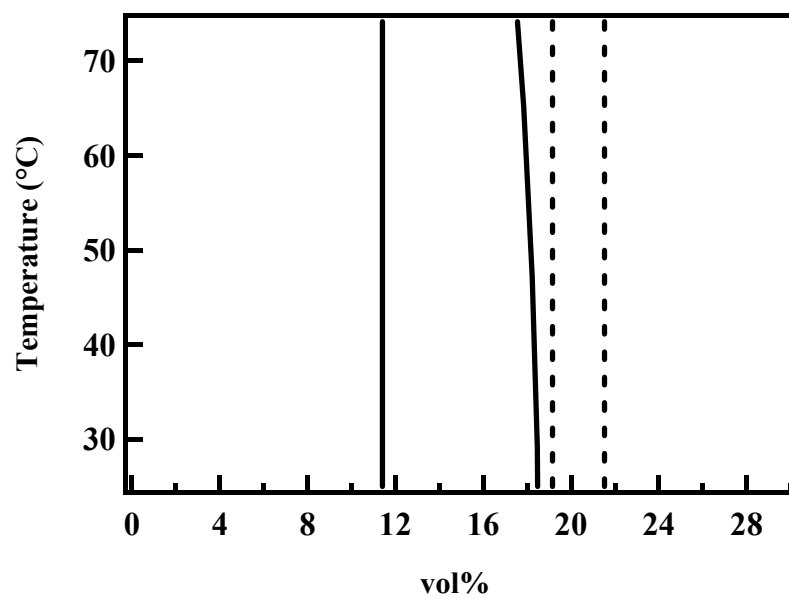


Figure 3



References

-
- ¹ L. Onsager, Ann. N. Y. Acad. Sci. **51**, 627 (1949).
- ² P. J. Flory, G. Ronca, Mol. Cryst. Liq. Cryst. **54**, 289 (1979); **54**, 311 (1979).
- ³ E. A. DiMarzio, J. Chem. Phys. **35**, 658 (1961).
- ⁴ M. Warner, P. J. Flory, J. Chem. Phys. **73**, 6327 (1980).
- ⁵ A. R. Khokhlov, A. N. Semenov, J. Statis. Phys. **38**, 161 (1985)
- ⁶ S. Fraden, G. Maret, D. L. D. Caspar, R. B. Meyer, Phys. Rev. Lett. **63**, 2068, (1989).
- ⁷ J. Lapointe, D. A. Marvin, Mol. Cryst. Liq. Cryst. **19**, 269 (1973).
- ⁸ J.-C. P. Gabriel, P. Davidson, Adv. Mat. **12**, 9 (2000).
- ⁹ P. A. Buining, H. N. W. Lekkerkerker, J. Phys. Chem., **97**, 11510 (1993).
- ¹⁰ L.-S. Li, J. Walda, L. Manna, A. P. Alivisatos, Nano Lett. **2**, 557 (2002).
- ¹¹ L.-S. Li, J. Hu, W. Yang, A. P. Alivisatos, Nano Lett. **1**, 349 (2001).
- ¹² J. Hu, L.-S. Li, W. Yang, L. Manna, L.-W. Wang, A. P. Alivisatos, Science **292**, 2060 (2001).
- ¹³ J. Seelig, Quart. Rev. Biophys. **10**, 353 (1977).
- ¹⁴ M. L. Kaplan, F. A. Bovey and H. N. Cheng, Anal. Chem. **47**, 1703 (1975).
- ¹⁵ C. Ammann, P. Meier, A. E. Merbach, J. Magn. Reson., **46**, 319 (1982).
- ¹⁶ L.-S. Li, A. P. Alivisatos, Adv. Mat. **15**, 408 (2003).
- ¹⁷ S.-D. Lee, J. Chem. Phys. **87**, 4972 (1987).
- ¹⁸ P. Bolhuis, and D. Frenkel, J. Chem. Phys. **106**, 666 (1998).
- ¹⁹ P. G. Bolhuis, A. Stroobants, D. Frenkel, H. N. W. Lekkerkerker, J. Chem. Phys. **107**, 1551 (1997).
- ²⁰ W. M. Gelbart, B. A. Baron, J. Chem. Phys. **66**, 207 (1977).

-
- ²¹ M. A. Cotter, J. Chem. Phys. **66**, 1098 (1977).
- ²² M. A. Cotter, in *The Molecular Physics of Liquid Crystals*, Ed. G. R. Luckhurst and G. W. Gray, Academic Press: London, 181 (1979).
- ²³ E. Rabani, B. Hetényi, B. J. Berne, L. E. Brus, J. Chem. Phys. **110**, 5355 (1999).
- ²⁴ E. Rabani, J. Chem. Phys. **115**, 1493 (2001).
- ²⁵ L.-S. Li, A. P. Alivisatos, Phys. Rev. Lett. **90**, 097402 (2003).
- ²⁶ P. van der Schoot, T. Odijk, J. Chem. Phys. **97**, 515 (1992).
- ²⁷ G. Ge, L. Brus, J. Phys. Chem. B **104**, 9573 (2000).
- ²⁸ O. Pelletier, P. Davidson, C. Bourgaux, J. Livage, Europhys. Lett. **48**, 53 (1999).